BIOCHEMISTRY
including biophysical chemistry & molecular biology
Article

Biochemistry **2010,** *49,* 5097–5108 5097
DOI: 10.1021/bi100410q

Understanding the Binding of Procyanidins to Pancreatic Elastase by Experimental and Computational Methods[†]

Natércia F. Brás,[‡] Rui Gonçalves,[§] Pedro A. Fernandes,[‡] Nuno Mateus,[§] Maria João Ramos,[‡] and Victor de Freitas*[,§]

[‡]*REQUIMTE and* [§]*Centro de Investigação em Química, Departamento de Química, Faculdade de Ciências, Universidade do Porto, Rua do Campo Alegre, 687, 4169-007 Porto, Portugal*

Received March 16, 2010; Revised Manuscript Received April 29, 2010

ABSTRACT: Human diets are rich in secondary metabolites such as polyphenols. These compounds perform a wide range of crucial functions in biological systems and are of great interest for the pharmaceutical and food industries. In this work, the binding mode of the natural polyphenolic compounds from grape seed on the porcine pancreatic elastase surface was studied by experimental and computational methods. Fluorescence quenching, circular dichroism, nephelometry, dynamic light scattering (DLS), molecular docking, and molecular dynamics simulation studies were performed. A decrease in fluorescence intensities was observed with addition of increasing polyphenol concentrations. The order of binding ability obtained was oligomeric fraction of procyanidins (OFP) > tetramer > trimer > dimer B3 procyanidins. Thus a relationship between higher molecular weight and binding ability was observed. The interaction between these molecules and the enzyme occurs by a static mechanism, as inferred from the high apparent fluorescence and bimolecular quenching constants. A blue shift in the maximal emission wavelength could be seen, which indicates that the tryptophan residues acquire a more hydrophobic character upon procyanidin binding. Molecular docking and dynamics simulations also demonstrate that the SASA (solvent-accessible surface area) values of tryptophans decrease with the binding of these compounds, preventing the accessibility of water molecules, which agrees with the referred blue shift. Circular dichroism studies indicate a decrease in α-helix content, followed by an increase in the *β*-sheet component of secondary structures of this enzyme. DLS and nephelometry techniques also indicate a relationship between large procyanidins and aggregate formation ability.

Polyphenol compounds possess many beneficial pharmacological properties, such as having antimutagenic and anticancerogenic effects as well as being natural antioxidants for the food industry (*1*−*3*). Dietary tannins can be subdivided in two broad classes, condensed (proanthocyanidins, which are flavan-3-ol units with various degrees of substitution and polymerization) and hydrolyzable tannins (gallic or ellagic esters of glucose) (*4*−*6*). Various studies have demonstrated that the large structures of condensed tannins are poorly absorbed in the intestine and remain in the digestive tract for a long time (*7*). Therefore, these large polyphenols can react and bind to proteins, acting as complexation or precipitation agents (*4*, *5*). It was also verified that the complexation performed by these tannins could denature digestive enzymes and lead to the loss of their catalytic activity, reducing food digestibility (*8*). On the other hand, it is known that some polyphenols may inhibit the activity of proteolytic enzymes, which have crucial therapeutic effect on disease processes, such as bacterial colonization, inflammation, angiogenesis, tumor invasion, and metastasis (*9*). Although various studies describe disease prevention by polyphenols, the exact mechanism by which this occurs is not clarified. It was suggested that the interactions of polyphenols/proteins may be governed by noncovalent binding, involving hydrogen bonds and van der Waals interactions established preferentially with the side chains of proline, histidine, arginine, and phenylalanine residues (*5*). All of these hydrophilic and hydrophobic interactions could result in insoluble aggregates that precipitate and prevent the enzymatic activity of proteins (*8*).

Polyphenol complexation and aggregation with proteins have been largely studied in solution by diverse techniques such as NMR spectroscopy (*10*), microcalorimetry (*11*), protein precipitation (*8*), front analysis capillary electrophoresis, turbidity (*12*), nephelometry (*8*), dynamic light scattering, circular dichroism (*13*−*18*), and fluorescence quenching (*5*). However, the interactions established between phenolic compounds and the porcine pancreatic elastases (PPE)[1] have never been studied. Pancreatic elastase is a serine protease secreted into the small intestine and is essential for digestion of a wide variety of protein substrates including the connective tissue protein elastin (*19*). This enzyme (E.C. 3.4.21.36) is composed by 240 amino acids in its active state and possesses a conserved active site catalytic triad formed by a serine, histidine, and aspartate residue (*20*). Structurally, this digestive enzyme is similar to the polymorphonuclear neutrophil elastase, which is involved in phagocytosis processes and controls

[†]This research was supported by research project grant (PTDC/AGR-ALI/67579/2006) funding from FCT (Fundação para a Ciência e Tecnologia) from Portugal. N.F.B. and R.G. thank FCT for Ph.D. grants (SFRH/BD/31359/2006 and SFRH/BD/38814/2007, respectively).

*To whom correspondence should be addressed. E-mail: vfreitas@fc.up.pt. Tel: +351 220 402 558. Fax: +351 402 659.

[1]Abbreviations: DLS, dynamic light scattering; OFP, oligomeric fraction of procyanidins; SASA, solvent-accessible surface area; CD, circular dichroism; PPE, porcine pancreatic elastase; MD, molecular dynamics; RMSD, root mean square deviation; RMSF, root mean square fluctuation.

Published on Web 05/20/2010

the proteolysis of elastic fibers during normal growth and remodeling (*9*). However, in pathological conditions, these enzymes cause an uncontrolled destruction of structural proteins, and severe diseases like pulmonary emphysema, acute pancreatitis, rheumatoid arthritis, and thrombosis can occur (*9*, *21*, *22*). The quantification of fecal elastase activity has been used has a predictor risk factor for the development of diseases such as osteoporosis (*23*) and diabetes mellitus (*24*).

Considering all these relevant medicinal importance, the structural similarity of both elastases and the fact that the PPE acts in the digestive tract, it is crucial to understand at the molecular level the binding of polyphenolic compounds to pancreatic elastase.

This work aims to explore the interaction of procyanidins from grape seed (dimer B3, trimer, tetramer, and one oligomeric fraction of procyanidins (OFP) with the average molecular weight of 1513) with PPE by biophysical methods, mainly fluorescence quenching of protein intrinsic fluorescence and circular dichroism (CD). Studies of protein precipitation with nephelometry and dynamic light scattering (DLS) techniques, as well as molecular docking and molecular dynamics simulations with these procyanidins bound to the enzyme, were also performed. In summary, a wide variety of techniques was used in order to explore the antinutritional property of the polyphenols on the digestive processes and the influence of the degree of polymerization of procyanidins to their ability to bind and precipitate this enzyme.

MATERIALS AND METHODS

Materials. Porcine pancreatic elastase was obtained from Sigma Aldrich and stored at −20 °C.

Synthesis and Isolation of Dimeric, Trimeric, and Tetrameric Procyanidins. The synthesis of procyanidin dimers, trimers, and tetramers followed the procedure described in the literature with slight modifications (*25*, *26*). For the synthesis of dimers, taxifolin (200 mg) and catechin (575 mg) were dissolved in ethanol under argon atmosphere (taxifolin/catechin ratio 1:3). The mixture was then treated by dropwise addition of sodium borohydride (in ethanol). The pH was then lowered to 4.5 by slowly adding CH_3COOH/H_2O 50% (v/v), and the mixture was allowed to stand under argon atmosphere for 30 min. The reaction mixture was extracted with ethyl acetate. After evaporation of the solvent, water was added, and the reaction mixture was passed through C18 gel, thoroughly washed with water, and recovered with methanol. The obtained fraction, after evaporation of methanol, was passed through a TSK Toyopearl HW-40(s) gel column (300 mm ×10 mm i.d., with 0.8 mL min^{-1} methanol as eluent) coupled to a UV−vis detector (Gilson 115). Several fractions were recovered and analyzed by ESI-MS (Finnigan DECA XP PLUS) yielding procyanidins with varying degrees of polymerization. Procyanidin methanolic solutions were mixed with water, the methanol was evaporated, and the procyanidins were freeze-dried for storage. For the production of trimer and tetramer the ratio of taxifolin to catechin were changed to 1:1 and 1:0.5, respectively, to favor the more polymerized products.

Oligomeric Procyanidin Fraction. Oligomeric procyanidins were obtained as described in the literature (*27*). *Vitis vinifera* grape seeds were extracted in ethanol/water/chloroform (1:1:2). The hydroalcoholic phase was extracted with ethyl acetate and evaporated, yielding a residue comprised of monomeric and oligomeric procyanidins. This residue was fractionated through a TSK Toyopearl HW-40(s) gel column (100 mm ×10 mm i.d., with 0.8 mL min^{-1} methanol as eluent) producing four fractions. Fractions 0 and I were obtained after elution with 99.8% (v/v) methanol during 1 and 5 h, respectively (cumulative time); fraction II was obtained after elution with methanol/CH_3COOH 5% (v/v) during the next 14 h; fraction III was obtained after elution with methanol/CH_3COOH 10% (v/v) during the next 8 h. Fractions were mixed with deionized water and freeze-dried. The procyanidin composition of each fraction was determined through ESI-MS (Finnigan DECA XP PLUS) as described elsewhere (*28*). Fraction I contains procyanidin trimer and tetramer and its galloyl derivatives (mean MW = 950); fraction II contains procyanidin pentamer and the galloyl derivative (mean MW = 1513); fraction III contains procyanidin pentamer digalloyl, procyanidin tetramer tetragalloyl, procyanidin hexamer galloyl, procyanidin heptamer, and the galloyl derivative (mean MW = 2052). The mean molecular weight of fractions was determined based on the relative abundance of each flavanol in the fraction. Fraction II was used in this study since it is simultaneously one of the most reactive with proteins (*29*) and the one obtained in largest quantity.

Fluorescence Quenching. A Perkin-Elmer LS 45 fluorometer was used for fluorescence quenching measurements. The excitation wavelength (λ_{ex}) was set at 290 nm, and the emission was recorded from 200 to 800 nm (both slits were 10 nm). The only exception occurs for the dimers B3 because these compounds possess strong intrinsic fluorescence at this λ_{ex}; therefore, the samples with these procyanidins were set at 305 nm. At this value, the intrinsic fluorescence emitted by dimers B3 is smaller than that one emitted by the indole groups of tryptophan. Therefore, a blank was made for each concentration, in which only the phosphate buffer replaced protein solution and all spectra of each solution were automatically corrected, subtracting the spectra of the respective polyphenol. The experiments were performed in 0.1 M phosphate buffer with a pH of 7.0. Stock solutions of PPE (0.5 mg/mL) and polyphenols such as dimers B3, trimers, tetramers, and the oligomeric fraction (procyanidin pentamers and galloyl derivatives) were prepared in phosphate buffer. All solutions were carefully filtered (0.45 μm). In several 2 mL microtubes, a fixed volume of elastase stock solution was mixed with different volumes of polyphenol stock solutions (from 0 to 160 μL) in order to give final concentrations of polyphenols in the range of 0−600 μM. The tubes were vortexed for 10 s and allowed to react for 1 h. After this, the solutions were transferred to the fluorometer cell where the emission spectra were measured. Between each measurement, the cell was washed three times with water. The blank spectrum was automatically subtracted from the emission spectrum of the corresponding solution. All experiments were performed in triplicate.

CD Measurements. Far-ultraviolet absorption (UV) CD of the samples was recorded in the range of 190−240 nm in 0.05 M phosphate buffer at a protein concentration of 10 μM (0.25 g/L) using a Jasco J 715 spectropolarimeter. The parameters were set as follows: step resolution, 1 nm; speed, 20 nm/min; bandwidth, 1 nm; response, 4 s; and sensitivity, 200 mdeg. A quartz cell having a 0.1 cm path length was used for the measurements. The concentration of each polyphenolic compound used was 10 μM. For baseline correction, CD spectra of buffer and solutions containing variable concentrations of polyphenols were collected and were subtracted from each sample spectra. Three scans were

accumulated for each spectrum. CD spectra in near-UV (240−300 nm) were measured in similar conditions to monitor the changes in tertiary structure after the addition of the phenolic compounds. Parameters were set similar to the CD spectra in far-UV; the only exception is the path length that was 1 cm. The secondary structure was determined using DICHROWEB (*30*), an online server for protein secondary structure analyses from CD spectroscopic data.

Nephelometry Measurements. The nephelometry experiments were conducted in the same manner as the fluorescence quenching assays except for the detection method. During nephelometry a Perkin-Elmer LS 45 fluorometer was used as a 90° light scattering photometer; both excitation and emission wavelengths selected were the same (400 nm), enabling the determination of light scattered by particles in solution. At this wavelength, protein and procyanidins do not absorb the incident light. A relative aggregation value (%) was calculated for each experiment as the ratio between the scatter intensity of the measured sample and that of the most turbid sample.

Dynamic Light Scattering. Both the size and the total number of aggregates present in solution were determined by dynamic light scattering (DLS) using a Zetasizer Nano ZS (Malvern). In this device the sample solution is illuminated by a 633 nm laser, and the intensity of light scattered at an angle of 173° is measured by an avalanche photodiode. This technique measures fluctuations in the intensity of scattered light when particles undergo Brownian motion. The analysis of these fluctuations enables the determination of the diffusion coefficients of particles, which are converted into a size distribution. This analysis provides information concerning particle size (obtained by the parameter number) and the amount of scattered light (count rate). Different volumes of procyanidin fraction stock solution in phosphate buffer were mixed with a fixed volume of PPE stock solution and allowed to react for 1 h. After this, the microtube was shaken, its content was transferred to a DLS plastic disposable cell, and the DLS measurement was performed. All solutions were thoroughly filtered through 0.2 μm disposable PTFE filters before mixing.

Statistical Analysis. All assays were performed in $n = 3$ repetitions. The statistical differences were evaluated using analysis of variance (ANOVA); the mean values were compared using a Tukey test, and all statistic data were processed using the SPSS software version 15.0 (SPSS Inc., Chicago, IL).

Computational Studies. The X-ray crystallographic structure of porcine pancreatic elastase was obtained from the Protein Data Bank (1QNJ code at 1.1 Å of resolution) (*20*). Various studies have shown the existence of conserved water in the elastase structure (*31*−*33*). In order to include these conserved crystallographic water molecules in the system, each water molecule that was buried inside the system or forms at least one H bond with the enzyme was maintained. This procedure led us to keep 80 of the water molecules of the crystallographic file and delete the others. All hydrogen atoms were added, taking into account all residues in their physiological protonation state. In order to release the bad contacts in the crystallographic structure, the protein was minimized in three stages during the initial geometry optimization. First, only the hydrogen atoms were minimized; in the second stage, the backbone was also minimized; and finally, the entire system was minimized. About 1500 steps were used for each stage, with the first 500 steps performed using the steepest descent algorithm and the remaining steps carried out using conjugate gradient. A dimer B3, trimer, and tetramer molecules were initially docked into the structure of the unligated protein. The docking procedure was made with GOLD (*34*), a program that predicts the binding modes of small molecules into protein binding sites. The program is based on a genetic algorithm that is used to place different ligand conformations in the protein binding site, recognized by a fitting points strategy. Three scoring functions are a posteriori available to rank the obtained solutions. As the docking accuracy obtained with all scoring functions is similar, and the ChemScore is up to three times faster when compared with the other, we have used this scoring function (*35*). Taking into account the lack of information about the polyphenol-binding mode to the elastase surface, the docking protocol was performed with a distance constraint (3.0−4.0 Å) between a carbon atom of the indole group present in Trp38 and a carbon atom of the A ring of each procyanidin studied. This constraint was performed because the fluorescence quenching studies have shown that the procyanidins interact with elastase close to the tryptophan residues. The best docking solutions were taken as starting structures for the subsequent minimizations and molecular dynamics (MD) simulations. To calculate the optimized geometries and electronic properties of all procyanidin molecules, to be used later in the parametrization of these compounds, we used the Gaussian 03 suite of programs (*36*) and performed restricted Hartree−Fock (RHF) calculations, with the 6-31G(d) basis set. The atomic charges were calculated using RESP (*37*). This methodology was chosen to be consistent with that adopted for the parametrization process in Amber 8.0 software (*38*). Molecular dynamics (MD) simulation was performed, with the parametrization adopted in Amber 8.0 using the Amber 1999 force field (parm99) for the protein and the GAFF, a general force field for small organic molecules, for the ligands. In these simulations, an explicit solvation model with preequilibrated TIP3P water molecules was used, filling a truncated octahedral box with a minimum 12 Å distance between the box faces and any atom of the protein. Each structure was minimized in two stages: first, the protein was kept fixed and only the position of the water molecules and counterions was minimized; in the second stage, the full system was minimized. Subsequently, a 500 ps equilibration followed by a 5 ns production MD simulation was carried out, starting from the optimized structure. The Langevin temperature equilibration scheme was used as well as constant volume and periodic boundary conditions (*39*). MD simulation was carried out using the Sander module, implemented in the Amber 8.0 simulations package (*40*), with the Cornell force field (*41*). Bond lengths involving hydrogens were constrained using the SHAKE algorithm(*42*), and the equations of motion were integrated with a 2 fs time step using the Verlet leapfrog algorithm. The nonbonded interactions were truncated with a 12 Å cutoff. The temperature of the systems was regulated to be maintained at 310.15 K. All of the MD results were analyzed with the Ptraj module of Amber 8.0.

RESULTS AND DISCUSSION

Fluorescence Quenching of the Protein Intrinsic Fluorescence. The fluorescence quenching method can be very helpful for understanding, at a molecular level, the binding affinity between the elastase and the polyphenol compounds, which can be at the origin of their poorly understood antinutritional effect. Therefore, the conformational change of elastase was evaluated by the measurement of the intrinsic fluorescence intensity of the tryptophan residues before and after the addition

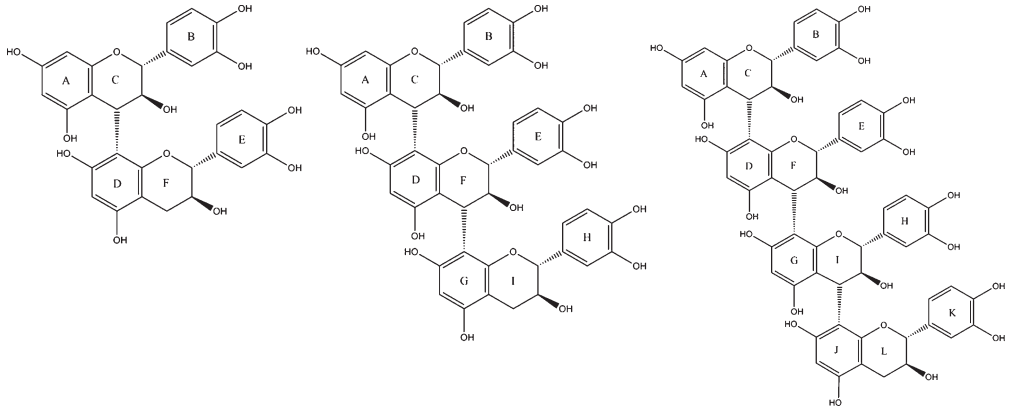

FIGURE 1: Representation of the dimer B3, trimer, and tetramer structures.

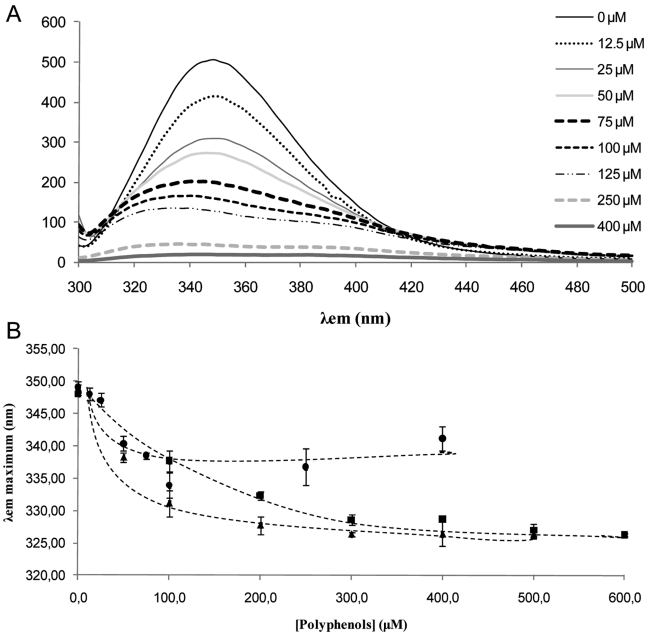

FIGURE 2: (A) Emission spectra of PPE (2 μM) at $\lambda_{ex} = 290$ nm (pH 7.0) in the presence of increasing concentrations of the oligomeric fraction of procyanidins (OFP). (B) λ_{em} maximum values obtained during the tryptophan fluorescence quenching of PPE (2 μM) at pH 7.0 in the presence of different concentrations of polyphenols: (■) trimer, (▲) tetramer, and (●) OFP.

of several procyanidins. The compounds studied were the dimer B3, trimer, tetramer, and one oligomeric fraction of procyanidins (OFP) with the higher average molecular weight (ca. 1513). The structures of the first three isolated procyanidins are represented in Figure 1.

Fluorescence measurements give information about the molecular environment around the chromophore molecule. In general, changes in the emission spectrum of tryptophan indicate protein conformational transitions, subunit association, substrate binding, or protein denaturation (*5*). Figure 2A shows the fluorescence emission spectra (λ_{ex} = 290 nm) obtained for elastase at pH 7.0 with the addition of the oligomeric fraction of procyanidins. A decrease in the fluorescence intensity caused by quenching was observed, as well as a shift of the maximum of emission wavelength (λ_{em}) to the left side, i.e., lower values of λ_{em} (Figure 2B). Similar reductions in the fluorescence intensity were observed for all procyanidins studied; however, the addition of dimer B3 did not modify significantly the λ_{em} values. The dominant fluorophore in proteins is the indole group of tryptophan, which absorbs close to 280 nm and emits near 340 nm. The observed λ_{em} for elastase in the absence of polyphenols is ca. 350 nm. As is possible to observe in Figure SI-1 in Supporting Information, PPE possesses 240 amino acids forming a single polypeptide and contains seven tryptophan residues with intrinsic fluorescence. These residues are located in different regions of the globular protein and thus are in distinct environments with different access to the quencher. The tryptophans in positions 27, 38, 94, 172, and 237 are colored at green and located on the surface of the protein; therefore, they are exposed and accessible to the solvent aqueous with a hydrophilic environment. Oppositely, Trp51 and Trp141 are colored at orange and are to be found inside to the protein within a hydrophobic pocket. As previously said, when the procyanidins bound to elastase, a shift to smaller wavelengths (blue shift) in the fluorescence spectra was observed (Figure 2B). This suggests that these polyphenols bound to the protein close to the tryptophan residues for the quenching to occur and change the microenvironment around these residues, making it more hydrophobic. This occurs probably due to conformational changes on the tryptophan side chains or simply because procyanidins interact with the indole groups preventing their interaction with the solvent. The fact that the smaller dimers B3 did not change the maximum emission wavelengths indicates that these procyanidins are too small to cause any conformational changes or solvent exclusion. Figure 5 shows the extinction of PPE tryptophan fluorescence quenching at pH 7.0 by addition of all procyanidins studied. It is well-known that different structures of polyphenols cause different behavior and changes of the environment around the tryptophan residues. It was also previously reported in the literature that in general an increment on molecular weight of polyphenols increases the complexation and binding affinities of grape seed procyanidins to proteins. Analyzing our data, it was observed that the oligomeric fraction of procyanidins leads to total quenching, while the dimers B3 show the smallest value of quenching (24.1%). Both trimer and tetramer procyanidins possess a similar effect on PPE fluorescence, quenched ca. 60% (Figure SI-2 in Supporting Information), whereas did not reach zero over the range of the concentrations studied. Interestingly, the lower concentrations of tetramers show an increment in fluorescence, probably due a small modification in the microenvironment close to the tryptophan residues. Oppositely, higher concentrations of these polyphenols demonstrate that they are a good quencher and cause elevated extinction of fluorescence values.

It is known that the Stern−Volmer equation (eq 1) describes the fluorescence quenching processes, where F_0 and F are the

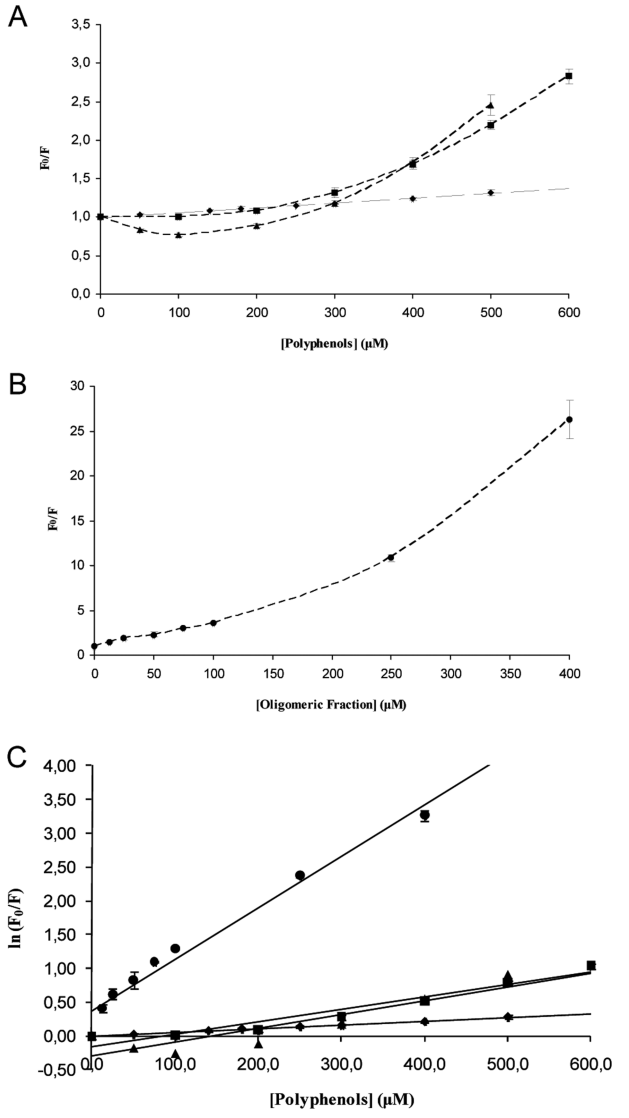

FIGURE 3: (A) Stern−Volmer plot describing tryptophan quenching of PPE (2 μM) at pH 7.0 in the presence of different concentrations of polyphenols: (◆) dimer B3, (■) trimer, and (▲) tetramer. (B) Stern−Volmer plot describing tryptophan quenching of PPE (2 μM) at pH 7.0 in the presence of different concentrations of OFP. Fluorescence emission intensity was recorded at λ_{ex} = 290 nm (except in dimers B3, for which the λ_{ex} = 305 nm), and the λ_{em} maximum occurred between 325 and 350 nm approximately. (C) Modified form of the Stern−Volmer plot in the presence of different concentrations of procyanidins: (■) trimer, $y = 1825x - 0.1575$; (▲) tetramer, $y = 2033.1x - 0.3002$, and (●) OFP, $y = 7626.2x + 0.3689$.

fluorescence intensities before and after the addition of the quencher (polyphenol compound), respectively. k_q is the bimolecular quenching constant, τ_0 is the lifetime of the fluorophore, specific of each fluorophore in the absence of the quencher, [Q] is the concentration of the quencher, and K_{SV} is the Stern−Volmer quenching constant. Using the Stern−Volmer equation, the K_{SV} is determined by linear regression of a plot of F_0/F against [Q].

$$F_0/F = 1 + kq\tau_0[Q] = 1 + K_{SV}[Q] \quad (1)$$

It is well-known that the fluorescence quenching processes can occur by a dynamic mechanism (with collisions induced), by a static mechanism (with a complex formation), or by the presence of a sphere of action, in which the quencher is adjacent to the fluorophore at the moment of excitation. This last mechanism assumes that when the fluorophore and quencher are close,

Table 1: Apparent Static (K) and Bimolecular (k_q) Quenching Constants for the Interaction of Dimer B3, Trimer, Tetramer, and the OFP with PPE at pH = 7.0[a]

procyanidins	K (M^{-1})	$k_q \times 10^{-11}$ (M^{-1} s^{-1})
dimer B3*	621 ± 52^a	2.39 ± 0.25^a
trimer	1806 ± 40^b	6.95 ± 0.15^b
tetramer	2027 ± 78^b	7.80 ± 0.30^b
OFP	7627 ± 304^c	29.30 ± 1.17^c

[a]Values with different superscript letters are significantly different ($P < 0.05$); values with the same superscript letters are not significantly different ($P > 0.05$).

quenching occurs before these molecules diffuse apart, instead of forming a ground-state complex as seen in the static mechanism. Panels A and B of Figure 3 show the Stern−Volmer plots for elastase fluorescence quenching by all procyanidins studied. Positive deviations were observed, which indicate large values of quenching. The plot obtained for dimers B3 is linear, indicating that only one type (dynamic or static) of quenching mechanism occurs. However, the Stern−Volmer plots for trimer, tetramer, and OFP exhibit an upward curvature, concave toward the y axis at high [Q]. These situations indicate that the quenching can occur by any one of the mechanisms (dynamic, static, or the presence of a sphere of action). In these situations, an apparent static quenching occurs, and the Stern−Volmer equation changed to the modified form (eq 2):

$$F_0/F = e^{K[Q]} \quad (2)$$

Using this equation, the apparent static constant (K) is determined by linear regression of a plot of $\ln(F_0/F)$ against [Q], and the bimolecular quenching constant (k_q) is calculated by the ratio between K_{SV} or K and τ_0. For the PPE enzyme, the lifetime of the fluorophore is approximately 2.60 ns (*43*). The K_{SV} and the bimolecular quenching constants for dimer B3 were obtained from the Stern−Volmer plot (Figure 3A), and both values are in Table 1. Figure 3C shows the modified form of the Stern−Volmer plot in the presence of different concentrations of each procyanidin studied. In order to analyze the specific interactions that occurred between the elastase tryptophan (fluorophore) and trimer, tetramer, and the OFP (quenchers), the apparent static Stern−Volmer (K) and bimolecular quenching constants were also calculated and are presented in Table 1.

The order of the apparent static and bimolecular quenching constants obtained was OFP > tetramer > trimer procyanidins. Considering the higher values of apparent static constants, it was concluded that after addition of these procyanidins, a complex that does not display fluorescence after returning from the excited state may be formed between these polyphenols and elastase molecules.

Furthermore, the maximum value of bimolecular quenching constant possible for diffusion-limited quenching (dynamic mechanism) in water is $\sim 10^{10}$ M^{-1} s^{-1}. Therefore, it was observed that PPE quenching occurs due to specific interactions and for dimer B3, trimer, and tetramer the k_q constants are 100-fold higher than the maximum value of diffusion-limited quenching in water. In the oligomeric fraction case, this k_q constant increases to 200-fold higher. Therefore, a complex formation between this enzyme and these procyanidin compounds was confirmed, which affects the tryptophan's microenvironment and is suggested by the static mechanism.

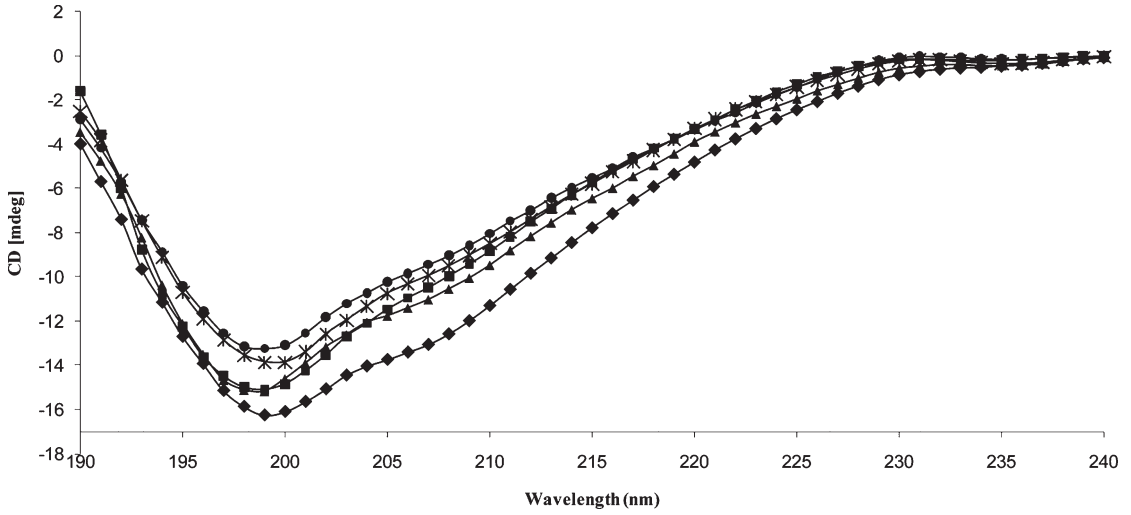

FIGURE 4: Far-UV circular dichroism spectra of elastase (10 μM) (◆) and its complexes with dimer B3 (■), trimer (▲), tetramer (*), and OFP (●) at pH 7.0 with protein:ligand ratio at 1:1 and 5 mM phosphate buffer.

It was observed that the K and k_q constant values obtained for the oligomeric fraction are much higher than the ones obtained for the other condensed tannins, which indicates a higher affinity of large procyanidins to elastase. As referred in the methodologies, the OFP used in this work contained procyanidin pentamers and galloyl derivatives. Previous studies have shown that the galloyl groups greatly contribute to a high binding activity toward proteins, showing unusually elevated values of apparent static quenching constant. The binding affinity for this oligomeric fraction is so high because each galloyl group provides three hydroxyl groups and a benzene ring, which can establish short hydrogen bonds and hydrophobic effects to the protein groups and improve the binding. These strong interactions could be responsible for the occurrence of the static mechanism instead of the dynamic one. The apparent Stern−Volmer quenching constants obtained for dimer B3, trimer, and tetramer indicate that the binding affinity to PPE increases with the molecular weight of procyanidins. This occurs due to the increment of aromatic rings and hydroxyl groups, with more catechin units available to form hydrophobic and hydrophilic bonds with the protein.

The three-dimensional structure of PPE present in Figure SI-1 in Supporting Information indicates that this enzyme has a pocket where it cleaves the peptide bonds and various loops with some flexibility. These loops allow the formation of diverse cavities, which could accommodate a range of ligands, and these various binding sites could be responsible for the high affinity observed for the large procyanidins that would act as multidentate ligands. Various studies have suggested that polyphenols bind preferentially to side chains of proline, histidine, arginine, and phenylalanine residues (*5*). However, the majority of studies point out the prolines as the most important binding site. PPE has seven proline residues distributed along its surface, allowing various binding sites around the enzyme in which a range of procyanidins could bind. Considering that the K constants correspondent to a binding affinity, our results agree with previous studies that suggest that the specificity of polyphenol−protein interactions depend to the size, structure, and charge of procyanidin and protein molecules.

Circular Dichroism. In order to understand the changes in elastase structure caused by the procyanidin addition, circular dichroism studies were performed. Far-UV CD spectra were conducted to evaluate the influence of procyanidin binding on the secondary structure of elastase. CD spectra of elastase exhibit two negative bands in the ultraviolet region at 199 and 208 nm as shown in Figure 4. These are characteristic of the natively unfolded protein and α-helical structure, respectively (*17*, *44*). CD spectra were analyzed by DICHROWEB (*30*), an online server for protein secondary structure analyses from CD spectroscopic data. Elastase belongs to a serine protease family, and its structure is highly similar to α-chymotrypsin and trypsin. Therefore, analyzing the X-ray structure of elastase it was observed that it consists of distorted antiparallel pleated sheets, forming very short irregular strands. In general, the β-sheet shows a CD band at 210−220 nm; however, in that case, these irregular strands could cause the negative CD band to shift from the ideal β-sheet position toward the 200 nm region (*44*).

Table 2: Secondary Structure Analysis of Free Elastase (10 μM) and Complexed with All Procyanidins Studied with Protein:Ligand Ratio at 1:1 Determined by CD Technique

	α-helix (%)	β-sheet (%)	β-turn (%)	random coil (%)
elastase	8.4	36.8	13.8	41.0
elastase:dimer B3	6.0	39.4	13.6	41.0
elastase:trimer	6.8	38.3	13.9	41.0
elastase:tetramer	6.1	39.2	13.5	41.2
elastase:OFP	6.1	39.9	13.4	40.6

Procyanidins interact with circularly polarized light, resulting in a non-null spectrum. It is relevant to notice that the CD spectra of the isolated procyanidins could be different from the CD spectra of the same procyanidins close to the protein elastase. However, considering the impossibility to confirm this fact, the CD spectrum of each procyanidin was removed by recording independently the spectrum of each compound alone in phosphate buffer. In Figure 4, a slight deviation from the native curve was observed, indicating that the binding of procyanidins to elastase results in perturbation of the protein secondary structure upon complexation. Table 2 shows the secondary structure distribution according to the CONTIN method, and it was found that the α-helix content of elastase decreases from 8.4% to a minimum of 6.0% upon binding the different procyanidin molecules. Furthermore, the curve-analyzing algorithm indicates

a slightly increase, from 36.8% to a maximum of 39.9%, in the percentage of β-sheet structure with the addition of these compounds. Oppositely, significant conformational changes in the unordered β-turn and random coil structures of the protein were not verified. Therefore, it is evident that the binding of procyanidins to elastase just causes small conformational changes on the secondary structure of protein. Considering that procyanidins with different molecular weight cause similar conformational changes on the secondary structure, it was concluded that the degree of polymerization did not influence these conformational modifications on elastase. In summary of these results, the binding of procyanidins to elastase leads a loss in its helical content, acquiring a higher percentage of pleated sheets.

The influence of the same procyanidin binding on the tertiary structure of elastase was evaluated by means of a near-UV study. At these wavelengths (240−300 nm), the chromophores are the aromatic amino acids (Trp, Tyr, and Phe) and disulfide bonds, and the CD signals they produce are sensitive to the overall tertiary structure of the protein. These curves change slightly upon complexation with all polyphenolic compounds tested (Figure SI-3 in Supporting Information), indicating some possible conformational restriction of the aromatic side chains (*13*, *17*). The CD spectra were especially influenced in the wavelength ranges of 240−250 and 280−290 nm, where the changes involved may be attributed specially to tryptophan and tyrosine side chains or to the three disulfide bonds present in elastase. This fact suggests that all procyanidins studied are close to these groups; however, this does not mean that these groups are directly involved in the binding of these polyphenols. On the other hand, the decrease observed in tryptophan's quenching upon procyanidin binding revealed that these compounds are close and interact with these amino acids, allowing a blue shift in the maximum λ_{em}. As previously referred, this deviation in the wavelength may occur due a conformational change in the side chain of tryptophan residues, which is in good agreement with the deviation observed in the near-UV-CD spectra obtained here.

Using CD studies, Rawel and colleagues obtained similar tridimensional structure changes of proteins (human serum albumin, bovine serum albumin, soy glycinin, and lysozyme) upon binding of phenolic compounds (chlorogenic, ferulic, and gallic acids, quercetin, rutin, and isoquercetin) (*17*). In summary, according to our CD studies, the noncovalent binding of procyanidins to elastase has a measurable effect on the secondary structure of this protein, while causing few modifications in its tertiary structure.

Docking on the Elastase Surface and Molecular Dynamics Studies. A molecular dynamics simulation of 2 ns of elastase was performed. The solvent-accessible surface area (SASA) defines the surface area of a group that is to accessible to a solvent probe. The SASA values for all tryptophan residues during this MD simulation were calculated in order to know which tryptophan residue is most exposed to the solvent. As expected, the tryptophan numbers 27, 38, 94, 172, and 237, located on the surface of the protein, have shown higher values, i.e., 22.0 ± 4.7, 94.3 ± 4.0, 37.1 ± 5.6, 55.8 ± 9.8, and 49.1 ± 3.1 Å^2, respectively. The smaller values of SASA (8.0 ± 0.7 and 15.4 ± 4.4 Å^2) were obtained for Trp51 and Trp141, respectively. These last residues are located inside the protein, within a hydrophobic environment. Thus they are not accessible to the solvent. In the previous fluorescence quenching studies, it was verified that some procyanidin molecules interact with elastase close to the tryptophan residues. In order to understand these specific contacts, the binding of dimer B3, trimer, and tetramer molecules to a tryptophan located in the elastase surface (Trp38) was simulated with docking and molecular dynamics methodologies. This specific tryptophan was chosen because it is the most exposed to the solvent. A docking protocol, using a distance constraint between the Trp38 and each polyphenolic compound, was performed. The best docking solutions were used as starting structures for the subsequent 7 ns long MD simulations. Figure 5 shows the closest structure to the average structure of each complex studied. The root-mean-square deviation (RMSD) values for the protein backbone (Cα) and for each procyanidin during the MD simulation were obtained and are shown in Figure SI-4 in Supporting Information. According to the results above, it can be observed that both RMSD values obtained for the protein backbone and dimer B3/trimer/tetramer are minimal, which reveal higher equilibration and stability of each complex. However, it was also noticed a huge change in the RMSD values for dimer B3 and tetramer after 3 and 4 ns, respectively. Therefore, these polyphenols change from an initial conformation to another, suggesting two possible conformations for these complexes. However, in the second conformation, the procyanidin molecules are closer to Trp38 than in the first one; thus we have analyzed the last 3.5 ns of each simulation, while in the trimer case, the last 5 ns were analyzed. In order to acquire a measure of the movement of a subset of the system relative to the average structure over the whole simulation, the RMSF values were also calculated for the protein by residues and are shown in Figure SI-5 in Supporting Information. Analyzing these values it was possible to observe higher RMSF values for residues Gly18, Asn132, Asn133, Arg145, Thr146, and Asn147 and the three loops constituted by the 166−174, 184−188, and 217−224 residues. On the other hand, the RMSF values of the residues included in the 10 Å radius around Trp38 show higher values for Ser32−Thr41, Leu63−Val67, Leu73, Tyr82, Gly84, and Val85. Therefore, these groups are the ones that mostly modify their position during all simulations studied, and the higher flexibility of these amino acids may be responsible for the changes observed in circular dichroism data.

The RMSF values were also calculated for the procyanidin molecules and Trp38 by atoms. Therefore, it was verified that in dimer B3 case the carbon atoms belonging to the B ring, and the hydroxyl groups of the B and E rings are the ones with more flexibility during the MD simulation. It was also observed that the carbon atoms of the B and H rings, as well as the hydroxyl groups belonging to the E and I rings of trimer, are the ones with higher degree of flexibility, while in the tetramer case the hydroxyl groups of the B, E, H, and K rings have the highest RMSF values. Figure 6 shows the RMSF values obtained for each atom of Trp38, and we can see that atoms 12−22 (belongs to tryptophan rings) show lower values of RMSF when bound to trimer or tetramer compounds. This suggests that the flexibility of this residue drops considerably with the presence of large procyanidin molecules, probably due its strong packing and complexation.

As previously referred, the Trp38 is the most exposed to the solvent; thus the side chain of this amino acid interacts with water molecules. However, it was expected that the addition of procyanidin molecules and the binding of their hydrophobic rings to the hydrophobic indole group on Trp38 would prevent the accessibility of solvent molecules. Moreover, this residue acquires a more hydrophobic microenvironment and emits at smaller wavelengths, which agrees with the blue shift observed in

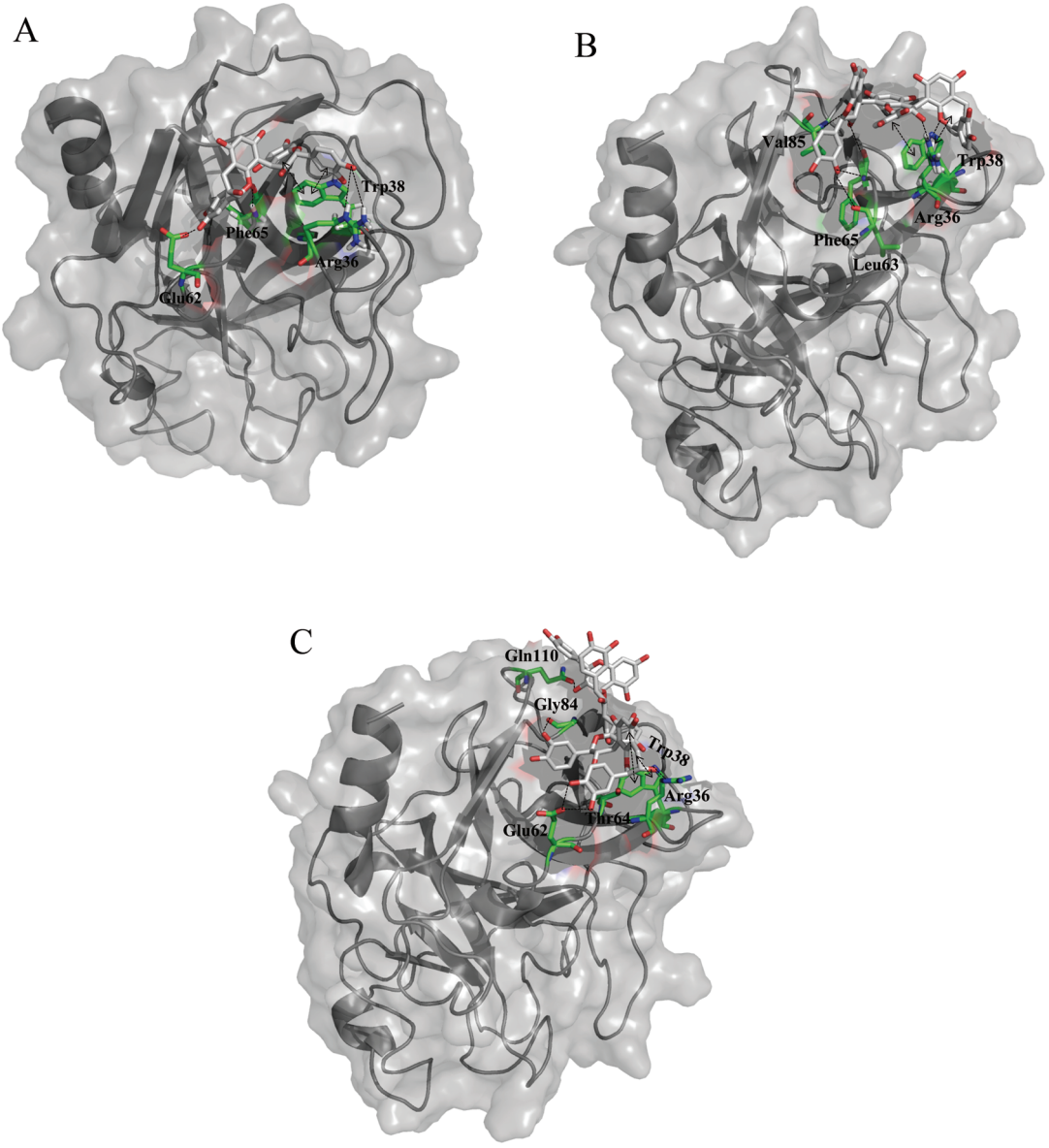

FIGURE 5: Representation of the closest structures of the average geometry to elastase:dimer B3 (A), elastase:trimer (B), and elastase:tetramer (C) complexes. Procyanidin molecules and the neighbor residues of elastase are represented by sticks in gray and green, respectively.

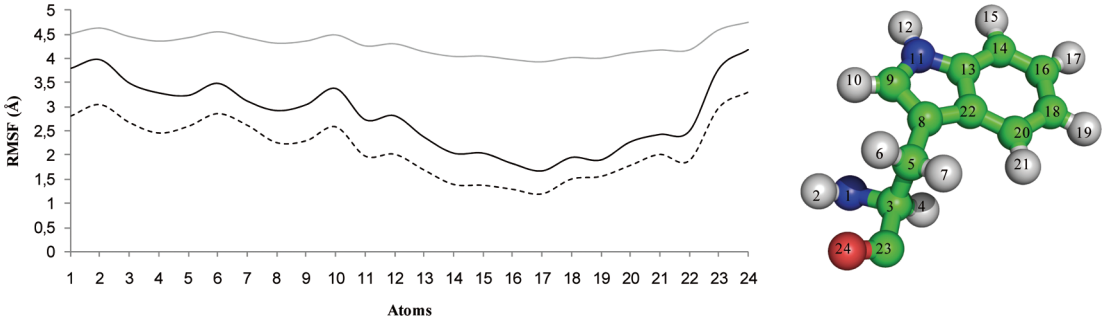

FIGURE 6: RMSF values obtained for Trp38 by atoms when complexed with dimer B3 (gray line), trimer (dashed line), and tetramer molecules (black line); representation of each number of Trp38.

the fluorescence data. The SASA value for Trp38 with each procyanidin bound was also calculated, and this value decreases from 94.3 ± 4.0 Å^2 (without procyanidins) to 86.7 ± 8.5, 90.3 ± 6.6, and 84.6 ± 3.2 Å^2 in the presence of the dimer B3, trimer, and tetramer compounds, respectively. Therefore, all of these values demonstrate that the environment around Trp38 acquires a character more hydrophobic after the binding of these procyanidin molecules. It is interesting to notice that the tetramer molecule is the one with the smaller SASA value, which indicates a higher protection and interaction with Trp38 performed by this large procyanidin. The interplanar distances between the plane defined by the indole group of Trp38 and the closest rings from

Table 3: Summary of Distances Involved in Main Interactions between Procyanidins (Dimer B3, Trimer, and Tetramer) and Neighboring Amino Acids on Elastase Surface

	elastase:dimer B3		elastase:trimer		elastase:tetramer	
residue	interaction	d (Å)	interaction	d (Å)	interaction	d (Å)
Arg36	NH ↔ OH (A ring)	4.04 ± 1.34	NH ↔ OH (F ring)	2.02 ± 0.24	NH ↔ OH (G ring)	2.62 ± 0.49
Trp38	NH ↔ OH (A ring)	3.79 ± 1.77	NH ↔ OH (D ring)	2.77 ± 0.42	apolar side chain ↔ plan of DF rings	
	apolar side chain ↔ plan of AC rings		NH ↔ O (I ring)	2.58 ± 0.55	apolar side chain ↔ plan of GI rings	
			apolar side chain ↔ plan of DF rings			
Glu62	COO^- ↔ HO (E ring)	1.64 ± 0.13			COO^- ↔ HO (K ring)	2.26 ± 0.89
	COO^- ↔ HO (E ring)	1.66 ± 0.13			COO^- ↔ HO (K ring)	2.29 ± 0.89
Leu63			CO ↔ HO (B ring)	3.71 ± 0.40		
Thr64					OH ↔ OH (I ring)	3.49 ± 1.58
Phe65	CO ↔ HO (A ring)	3.59 ± 1.41	NH ↔ OH (B ring)	2.06 ± 0.17		
			CO ↔ HO (C ring)	2.58 ± 0.55		
Gly84					NH ↔ OH (C ring)	2.20 ± 0.37
Val85			NH ↔ OH (C ring)	1.95 ± 0.15		
Gln110					CO ↔ HO (C ring)	2.04 ± 0.69

each procyanidin were also calculated for the first and the last 2 ns of each simulation after equilibration. In Figure 5A, the elastase:dimer B3 complex shows that this polyphenol has two hydrophobic rings close to the indole group. Therefore, it was observed that the average distances between the indole group and A and D rings of dimer B3 change from 10.9 ± 3.7 and 12.2 ± 3.6 Å in the first 2 ns to 6.2 ± 0.3 and 7.5 ± 0.9 Å, respectively, in the last 2 ns of MD simulation. In the elastase:trimer (Figure 5B) and elastase:tetramer (Figure 5C) complexes, there are also one and two hydrophobic rings close to the indole group, respectively. The average distance between the indole group and the A ring of trimer changes from 6.8 ± 0.6 Å to 6.5 ± 0.6 Å, while the average distances between the indole group and the A and F rings of tetramer change from 12.2 ± 0.8 and 12.3 ± 0.8 Å to 11.3 ± 0.5 and 11.3 ± 0.6 Å, respectively. All of these alterations in the average interplanar distances revealing a proximity of hydrophobic rings of each procyanidin to the side chain of the tryptophan studied consequently also indicate that this residue change to a more hydrophobic environment. In summary, these computational data suggest some conformational changes on Trp38 or in the neighbor amino acid side chains in order to acquire a most hydrophobic environment, which is in total agreement with the blue shift observed in the fluorescence data, as well as with the conformational changes of the aromatic side chains observed in the circular dichroism data.

Structural information on the elastase surface, in particular the hydrogen bonds established between the procyanidins molecules and the neighbor residues, as well as van der Waals contacts established between the polyphenolic rings and the aliphatic side chains, was analyzed and is shown in Table 3. It was seen that the main hydrogen interactions occur between the hydroxyl groups of procyanidins and the side chains of Arg36, Trp38, Glu62, Leu63, Thr64, Phe65, Gly84, Val85, and Gln110 residues present on the elastase surface. Both Arg36 and Trp38 are crucial to the binding of polyphenols due to the establishment of short interactions with all of the compounds studied. Furthermore, the indole group of this tryptophan establishes van der Waals interactions with some rings of each procyanidin, namely, perpendicular $\pi-\pi$ stacking with the plan defined by A and C rings of dimer B3 molecule, while in the trimer and tetramer compounds these vertical hydrophobic effects occurred with the plan defined by D and F rings. These hydrophobic contacts are crucial, contributing to the binding

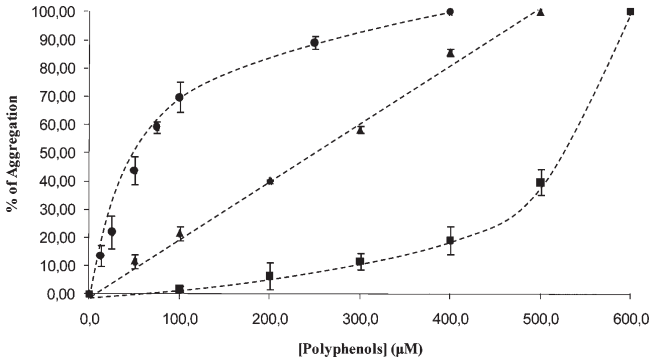

FIGURE 7: Changes in PPE (2 μM)/procyanidin aggregation intensity (turbidity obtained with nephelometry) by increasing concentrations of trimer (■), tetramer (▲), and OFP (●) in 0.1 M phosphate buffer at pH 7.0.

mode of procyanidins on the elastase surface, and allow the stabilization of each complex.

Elastase/Procyanidin Aggregate Formation and Measurements. The interaction of procyanidins and proteins leads to the appearance of macroaggregates resulting from the formation of cross-linked network structures that may precipitate. In order to determine the aggregate formation on a supramolecular level, the turbidity of PPE/procyanidin solutions was measured by nephelometry (Figure 7). This technique demonstrates an increment in protein aggregating ability with increasing concentration of procyanidins. However, our data show that the OFP induces a higher value of aggregation at much lower concentration (400 μM) than the trimer and tetramer procyanidins (500 and 600 μM, respectively). These concentrations correspond to the stoichiometric concentration between each procyanidin and PPE. Interestingly, the smallest dimer B3 procyanidin did not form aggregates probably due to the weak interactions established with the proteins or because their small size is unable to induce cross-links in elastase.

As this technique does not give information about the aggregate sizes, the average size was measured using dynamic light scattering (DLS). The technique uses the analysis of fluctuations in the intensity of scattered light to determine the diffusion coefficients of particles and translates these values into a size distribution. Although these results could be calculated using the particles that scatter more light (intensity) or the most abundant particles (number), herein the later distribution is more

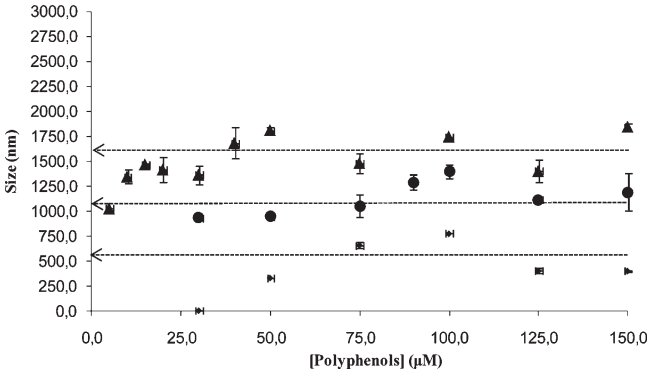

FIGURE 8: Changes in PPE (2 μM)/procyanidin aggregation size by increasing concentrations of trimer (◆), tetramer (■), and OFP (▲) in 0.1 M phosphate buffer at pH 7.0. The array indicates the mean size of aggregate for each procyanidin.

useful because the most abundant particles in solution are expected to be the formed aggregates. Figure 8 shows the size of aggregates formed in function to the trimer, tetramer, and the OFP concentrations. In the oligomeric fraction, the maximal size was readily attained for the lowest concentration of procyanidins, and after this, only a slight increase in size with concentration was observed. For tetramer, the mean maximal size was also obtained in the lowest concentrations; however, in this case the size of aggregates stabilizes with higher concentrations. In the case of aggregates with trimer, it was observed that their size directly increases with the concentration, attained a maximal size value, whereas to the highest concentrations a slight decrease in the size was observed. In general, these results suggest that these procyanidins form aggregates with elastase with mean specific sizes that do not change considerably after reaching a maximum despite further addition of procyanidins. It can be noticed that the mean sizes of aggregates formed by OFP (≈1550 nm) are higher than the ones formed by tetramer (≈1050 nm) and trimer (≈550 nm). This reveals the importance of increasing degrees of polymerization in the rise in the ability to aggregate with proteins and form structures with higher complexity. A direct relationship between the aggregate size and the polymerization degree of procyanidins was observed. These data seem to be in agreement with the ones obtained in fluorescence quenching studies in which the more polymerized procyanidins are shown to have more affinity to bind elastase molecules.

CONCLUSIONS

Fluorescence quenching studies have been performed to understand the procyanidin binding mode, and a decrease in fluorescence intensity with addition of increasing polyphenol concentrations was observed. Considering the high Stern−Volmer constant values obtained for the procyanidins studied, it was concluded that the interaction between these compounds and the elastase surface occurs by a static mechanism. The order of apparent quenching constants obtained was OFP > tetramer > trimer > dimer B3 procyanidins. It was verified that the binding capacity increases with increasing molecular weight. Therefore, the procyanidin fraction with highest average molecular weight possesses a higher ability to bind on elastase surface. It was concluded that more polymerized procyanidins establish stronger intermolecular interactions with the side chains of the residues present on elastase surface and thus have higher binding ability than the smaller ones. Furthermore, a blue shift in the maximal emission wavelength toward smaller values was observed, which indicates that the tryptophan residues acquire a larger hydrophobic character upon procyanidin complexation.

Circular dichroism reveals that elastase undergoes a small secondary structure change: its α-helix content decreases and the percentage of β-sheet structure increases. Near-UV spectra show that the tertiary structure of elastase undergoes a moderate structural loosening upon procyanidin complexation.

Molecular docking and dynamics simulations also demonstrate that short hydrogen bonds and van der Waals interactions established between the polyphenol groups and the side chains of residues present on the elastase surface stabilize and favor the binding mode of this procyanidin. It was also verified that SASA values of Trp38, located on the enzyme surface, highly decrease with the addition of the tetramer, indicating that this large procyanidin prevents the interaction with solvent, which is in good agreement with the blue shift observed in fluorescence data.

Finally, it was concluded that the interaction of procyanidins with elastase also allows the formation of insoluble aggregates detected by dynamic light scattering and nephelometry, and the size and number of these aggregates increase with higher concentrations and larger compounds.

Regarding the biological implications of such interactions, these results should be viewed from two different perspectives. First, from a biomedical point of view and taking into account the excessive fast-food consumption habits in industrialized countries, this work might provide a basis for drug development in the control of obesity and food-related disorders. As the enzyme used is a member of the serine protease family, this work might also provide insights on the development of serine protease inhibitors that may be used for the treatment of several diseases (pulmonary emphysema, acute pancreatitis, rheumatoid arthritis, and thrombosis). From a nutritional and food industry perspective the present study is crucial to explore the antinutritional effects caused by dietary polyphenols on digestive enzymes and the corresponding reduction of food digestibility and nutrient absorption.

Future work might involve the study of the interaction process by NMR techniques to determine not only the affinity of procyanidins for proteins but also the stoichiometry of the interaction. Site-directed mutagenesis could be used to identify which of the seven Trp residues are most affected by the interaction with procyanidins. It will also be relevant to determine what are the biological effects resulting from the interaction such as the inhibition of the enzyme activity.

ACKNOWLEDGMENT

The authors thank João Costa Pessoa and Isabel Correia at Instituto Superior Técnico for collaboration in the circular dichroism studies.

SUPPORTING INFORMATION AVAILABLE

Figure SI-1, representation of the porcine pancreatic elastase structure; Figure SI-2, tryptophan fluorescence quenching of PPE (2 μM) at pH 7.0; Figure SI-3, near-UV circular dichroism spectra of elastase and its complexes with dimer B3, trimer, tetramer, and OFP; Figure SI-4, RMSD values obtained for the elastase backbone and for each procyanidin; Figure SI-5, RMSF values obtained for the elastase by residues complexed with dimer B3, trimer, and tetramer molecules. This material is available free of charge via the Internet at http://pubs.acs.org.

REFERENCES

1. Daniel, K. G., Landis-Piwowar, K. R., Chen, D., Wan, S. B., Chan, T. H., and Dou, Q. P. (2006) Methylation of green tea polyphenols affects their binding to and inhibitory poses of the proteasome beta 5 subunit. *Int. J. Mol. Med. 18* (4), 625–632.
2. Pezzato, E., Sartor, L., Dell Aica, I., Dittadi, R., Gion, M., Belluco, C., Lise, M., and Garbisa, S. (2004) Prostate carcinoma and green tea: PSA-triggered basement membrane degradation and MMP-2 activation are inhibited by (−)epigallocatechin-3-gallate. *Int. J. Cancer 112* (5), 787–792.
3. Xue, Z. P., Feng, W. H., Cao, J. K., Cao, D. D., and Jiang, W. B. (2009) Antioxidant activity and total phenolic contents in peel and pulp of Chinese jujube (*Ziziphus jujuba* Mill) fruits. *J. Food Biochem. 33* (5), 613–629.
4. Goncalves, R., Soares, S., Mateus, N., and De Freitas, V. (2007) Inhibition of trypsin by condensed tannins and wine. *J. Agric. Food Chem. 55* (18), 7596–7601.
5. Soares, S., Mateus, N., and De Freitas, V. (2007) Interaction of different polyphenols with bovine serum albumin (BSA) and human salivary alpha-amylase (HSA) by fluorescence quenching. *J. Agric. Food Chem. 55* (16), 6726–6735.
6. Mateus, N., Silva, A. M. S., Santos-Buelga, C., Rivas-Gonzalo, J. C., and de Freitas, V. (2002) Identification of anthocyanin-flavanol pigments in red wines by NMR and mass spectrometry. *J. Agric. Food Chem. 50* (7), 2110–2116.
7. McDougall, G. J., and Stewart, D. (2005) The inhibitory effects of berry polyphenols on digestive enzymes. *Biofactors 23* (4), 189–195.
8. de Freitas, V., Carvalho, E., and Mateus, N. (2003) Study of carbohydrate influence on protein-tannin aggregation by nephelometry. *Food Chem. 81* (4), 503–509.
9. Dell'Aica, I., Niero, R., Piazza, F., Cabrelle, A., Sartor, L., Colalto, C., Brunetta, E., Lorusso, G., Benelli, R., Albini, A., Calabrese, F., Agostini, C., and Garbisa, S. (2007) Hyperforin blocks neutrophil activation of matrix metalloproteinase-9, motility and recruitment, and restrains inflammation-triggered angiogenesis and lung fibrosis. *J. Pharmacol. Exp. Ther. 321* (2), 492–500.
10. Baxter, N. J., Lilley, T. H., Haslam, E., and Williamson, M. P. (1997) Multiple interactions between polyphenols and a salivary proline-rich protein repeat result in complexation and precipitation. *Biochemistry 36* (18), 5566–5577.
11. Frazier, R. A., Papadopoulou, A., Mueller-Harvey, I., Kissoon, D., and Green, R. J. (2003) Probing protein-tannin interactions by isothermal titration microcalorimetry. *J. Agric. Food Chem. 51* (18), 5189–5195.
12. Horne, J., Hayes, J., and Lawless, H. T. (2002) Turbidity as a measure of salivary protein reactions with astringent substances. *Chem. Senses 27* (7), 653–659.
13. Jobstl, E., O'Connell, J., Fairclough, J. P. A., and Williamson, M. P. (2004) Molecular model for astringency produced by polyphenol/protein interactions. *Biomacromolecules 5* (3), 942–949.
14. Maiti, T. K., Ghosh, K. S., and Dasgupta, S. (2006) Interaction of (−)-epigallocatechin-3-gallate with human serum albumin: Fluorescence, Fourier transform infrared, circular dichroism, and docking studies. *Proteins: Struct., Funct., Bioinf. 64* (2), 355–362.
15. Pascal, C., Pate, F., Cheynier, V., and Delsuc, M. A. (2009) Study of the interactions between a proline-rich protein and a flavan-3-ol by NMR: residual structures in the natively unfolded protein provides anchorage points for the ligands. *Biopolymers 91* (9), 745–756.
16. Pascal, C., Poncet-Legrand, C., Imberty, A., Gautier, C., Sarni-Manchado, P., Cheynier, V., and Vernhet, A. (2007) Interactions between a nonglycosylated human proline-rich protein and flavan-3-ols are affected by protein concentration and polyphenol/protein ratio. *J. Agric. Food Chem. 55* (12), 4895–4901.
17. Rawel, H. A., Meidtner, K., and Kroll, J. (2005) Binding of selected phenolic compounds to proteins. *J. Agric. Food Chem. 53* (10), 4228–4235.
18. Simon, C., Barathieu, K., Laguerre, M., Schmitter, J. M., Fouquet, E., Pianet, I., and Dufourc, E. J. (2003) Three-dimensional structure and dynamics of wine tannin-saliva protein complexes. A multitechnique approach. *Biochemistry 42* (35), 10385–10395.
19. Nadarajah, D., Atkinson, M. A. L., Huebner, P., and Starcher, B. (2008) Enzyme kinetics and characterization of mouse pancreatic elastase. *Connect. Tissue Res. 49* (6), 409–415.
20. Wurtele, M., Hahn, M., Hilpert, K., and Hohne, W. (2000) Atomic resolution structure of native porcine pancreatic elastase at 1.1 angstrom. *Acta Crystallogr., Sect. D: Biol. Crystallogr. 56*, 520–523.
21. Dell'Aica, I., Caniato, R., Biggin, S., and Garbisa, S. (2005) Matrix proteases, green tea, and St. John's wort: biomedical research catches up with folk medicine, in International Conference on Enzymes—Old Molecules with New Clinical Applications, Padova, Italy.
22. Sartor, L., Pezzato, E., Dell'Aica, I., Caniato, R., Biggin, S., and Garbisa, S. (2002) Inhibition of matrix-proteases by polyphenols: chemical insights for anti-inflammatory and anti-invasion drug design. *Biochem. Pharmacol. 64* (2), 229–237.
23. Teichmann, J., Lange, U., Hardt, P., Schnell-Kretschmer, H., Stracke, H., Bretzel, R. G., and Klor, H. U. (2001) Decreased pancreatic elastase I stool content: an independent risk factor of the osteoporosis in elderly women. *Bone 28* (5), S194–S194.
24. Rathmann, W., Haastert, B., Icks, A., Giani, G., Hennings, S., Mitchell, J., Curran, S., and Wareham, N. J. (2001) Low faecal elastase 1 concentrations in type 2 diabetes mellitus. *Scand. J. Gastroenterol. 36* (10), 1056–1061.
25. Geissman, T. A., and Yoshimura, N. N. (1966) Synthetic proanthocyanidin. *Tetrahedron Lett. 7* (24), 2669–2673.
26. Delcour, J. A., Ferreira, D., and Roux, D. G. (1983) Synthesis of condensed tannins. Part 9. The condensation sequence of leucocyanidin with (+)-catechin and with the resultant procyanidins. *J. Chem. Soc., Perkin Trans. 1,* 1711–1717.
27. de Freitas, V., Glories, Y., Bourgeois, G., and Vitry, C. (1998) Characterisation of oligomeric and polymeric procyanidins from grape seeds by liquid secondary ion mass spectrometry. *Phytochemistry 49* (5), 1435–1441.
28. González-Manzano, S., Mateus, N., de Freitas, V., and Santos-Buelga, C. (2008) Influence of the degree of polymerisation in the ability of catechins to act as anthocyanin copigments. *Eur. Food Res. Technol. 227* (1), 83–92.
29. Gonçalves, R., Soares, S., Mateus, N., and de Freitas, V. (2007) Inhibition of trypsin by condensed tannins and wine. *J. Agric. Food Chem. 55* (18), 7596–7601.
30. Whitmore, L., and Wallace, B. A. (2004) DICHROWEB, an online server for protein secondary structure analyses from circular dichroism spectroscopic data. *Nucleic Acids Res. 32*, W668–W673.
31. Geller, M., Swanson, S. M., and Meyer, E. F. (1990) Dynamic properties of the 1st steps of the enzymatic reaction of porcine pancreatic elastase (PPE). 2. Molecular-dynamics simulation of a Michaelis complex—PPE and the hexapeptide Thr-Pro-Nval-Leu-Tyr-Thr. *J. Am. Chem. Soc. 112* (24), 8925–8931.
32. Sreenivasan, U., and Axelsen, P. H. (1992) Buried water in homologous serine proteases. *Biochemistry 31* (51), 12785–12791.
33. Wilmouth, R. C., Edman, K., Neutze, R., Wright, P. A., Clifton, I. J., Schneider, T. R., Schofield, C. J., and Hajdu, J. (2001) X-ray snapshots of serine protease catalysis reveal a tetrahedral intermediate. *Nat. Struct. Biol. 8* (8), 689–694.
34. Jones, G., Willett, P., Glen, R. C., Leach, A. R., and Taylor, R. (1997) Development and validation of a genetic algorithm for flexible docking. *J. Mol. Biol. 267* (3), 727–748.
35. Verdonk, M. L., Cole, J. C., Hartshorn, M. J., Murray, C. W., and Taylor, R. D. (2003) Improved protein-ligand docking using GOLD. *Proteins: Struct., Funct., Genet. 52* (4), 609–623.
36. Frisch, M. J., Trucks, G. W., Schlegel, H. B., Scuseria, G. E., Robb, M. A., Cheeseman, J. R., Zakrzewski, V. G., Montgomery, J. A., Jr., Stratmann, R. E., Burant, J. C., Dapprich, S., Millam, J. M., Daniels, A. D., Kudin, K. N., Strain, M. C., Farkas, O., Tomasi, J., Barone, V., Cossi, M., Cammi, R., Mennucci, B., Pomelli, C., Adamo, C., Clifford, S., Ochterski, J., Petersson, G. A., Ayala, P. Y., Cui, Q., Morokuma, K., Malick, D. K., Rabuck, D. A., Raghavachari, K., Foresman, J. B., Cioslowski, J., Ortiz, J. V., Baboul, A. G., Stefanov, B. B., Liu, G., Liashenko, A., Piskorz, P., Komaromi, I., Gomperts, R., Martin, R. L., Fox, D. J., Keith, T., Al-Laham, M. A., Peng, C. Y., Nanayakkara, A., Gonzalez, C., Challacombe, M., Gill, P. M. W., Johnson, B., Chen, W., Wong, M. W., Andres, J. L., Gonzalez, C., Head-Gordon, M., Replogle, E. S., and Pople, J. A. (2003) Gaussian 03, Gaussian, Inc., Pittsburgh, PA.
37. Bayly, C. I., Cieplak, P., Cornell, W. D., and Kollman, P. A. (1993) A well-behaved electrostatic potential based method using charge restraints for deriving atomic charges—the Resp model. *J. Phys. Chem. 97* (40), 10269–10280.
38. Case, D. A., Cheatham, T. E., Darden, T., Gohlke, H., Luo, R., Merz, K. M., Onufriev, A., Simmerling, C., Wang, B., and Woods, R. J. (2005) The Amber biomolecular simulation programs. *J. Comput. Chem. 26* (16), 1668–1688.
39. Izaguirre, J. A., Catarello, D. P., Wozniak, J. M., and Skeel, R. D. (2001) Langevin stabilization of molecular dynamics. *J. Chem. Phys. 114* (5), 2090–2098.
40. Case, D. A., Darden, T. A., Cheatham, T. E., III, Simmerling, C. L., Wang, J., Duke, R. E., Luo, R., Merz, H. M., Wang, B., Pearlman, D. A., Crowley, M., Brozell, S., Tsui, V., Gohlke, H., Mongan, J.,

Hornak, V., Cui, G., Beroza, P., Schafmeister, C., Caldwell, J. W., Ross, W. S., and Kollman, P. A. (2004) AMBER 8, University of California, San Francisco.
41. Cornell, W. D., Cieplak, P., Bayly, C. I., Gould, I. R., Merz, K. M., Ferguson, D. M., Spellmeyer, D. C., Fox, T., Caldwell, J. W., and Kollman, P. A. (1995) A 2nd generation force field for the simulation of proteins, nucleic acids, and organic molecules. *J. Am. Chem. Soc. 117* (19), 5179–5197.
42. Ryckaert, J. P., Ciccotti, G., and Berendsen, H. J. C. (1977) Numerical integration of Cartesian equations of motion of a system with constraints—molecular dynamics of N-alkanes. *J. Comput. Phys. 23* (3), 327–341.
43. Prendergast, F. G., Lu, J., and Callahan, P. J. (1983) Oxygen quenching of sensitized terbium luminescence in complexes of terbium with small organic-ligands and proteins. *J. Biol. Chem. 258* (7), 4075–4078.
44. Simon, L. M., Kotorman, M., Garab, G., and Laczko, I. (2001) Structure and activity of alpha-chymotrypsin and trypsin in aqueous organic media. *Biochem. Biophys. Res. Commun. 280* (5), 1367–1371.